

Analyzing Process Related, In-Plane Mechanical Variation of High Density Fiber Boards (HDF) Across the Feed Direction

Jörn Rathke,^{a*} Martin Riegler,^a Martin Weigl,^a Ulrich Müller,^a and Gerhard Sinn^b

Mechanical properties of the core layer (in-plane) of high density fiberboards (HDF) were analyzed across the width of the board (*i.e.* across the feed direction). The tests were performed by means of a newly developed double cantilever I beam (DCIB) testing system, with analysis of internal bond strength and bending strength. The specimens were selected from a large-scale experiment in a central European HDF plant, including a completely different machine setting for each sample set. Homogeneous density and property distributions across the feed direction of the boards were generally assumed. During this trial the question arose as to whether processing leads to unequal mechanical properties across the feed direction. In total, 20 sample sets were tested longitudinally and laterally to the feed direction at eight measurement points, revealing 320 test specimens per testing procedure. In contrast to standard testing procedures, the specific fracture energy and the stress intensity factor revealed significant differences between the centre and the edge across the feed direction. This study revealed variations of mechanical properties across the width of the board using the DCIB approach.

Keywords: Bending strength; High density fiber board; Internal bond strength; Specific fracture energy; Stress intensity factor; Mechanic variation

Contact information: a: Wood K plus – Competence Centre for Wood Composites and Wood Chemistry Altenberger Straße 69, 4040 Linz, Austria; b: Department of Material Sciences and Process Engineering, Institute of Physics and Material Sciences, BOKU – University of Natural Resources and Life Sciences, Peter Jordan Straße 82, 1190 Vienna, Austria; *Corresponding author: j.rathke@kplus-wood.at

INTRODUCTION

In general, wood is a highly heterogeneous and complex material. This includes inhomogeneities such as fibers, knots, pores, pith, *etc.* In addition, processing parameters highly influence its mechanical properties. To overcome this drawback, wood can be fragmented into strands, particles, or fibers and reassembled by means of resin, pressure, and heat to obtain relatively homogeneous wood-based panels with customized properties. Besides the orientation and size of particles, the entire production process highly influences the board properties. In recent decades, the continuous hot pressing process has become the most widely used technology in the production of wood-based panels (Pereira *et al.* 2006). Pressing parameters (*i.e.*, temperature, time, press factor, pressure) impact the hardening behavior of resin, the plastification of the wood structure (Bouajila *et al.* 2005), and the density profile of the board (Dunky and Niemz 2002). In medium density or high density fiberboard (MDF/HDF) production processes, coupled physical, mechanical, and chemical phenomena influence the entire process and the final product. Numerous investigations have been performed to describe the correlation

between mechanical properties of fiberboards and resin content (Maxwell *et al.* 1984; Waters 1990; Roffael *et al.* 2003; Roffael *et al.* 2005), mat forming (Wang *et al.* 2001), pressing (Park *et al.* 1999; Carvalho *et al.* 2001; Cao *et al.* 2007), heat transfer (Park *et al.* 1999; Cao *et al.* 2007), and resin curing (Heinemann 2004; Walther 2006). To analyze board properties, the selection and preparation of specimens have to follow a precise procedure, regulated in EN 326-2. In particular, specimens have to be oriented longitudinally and laterally to the production direction to take production-based strength and density variations into account. The production of wood-based panels on a continuous hot press (Fig. 1a) leads to density variations across the width of the board (Fig. 1b). These variations can be caused either unintentionally or systematically, *e.g.*, by inducing a higher density toward the edge to keep the heat within the board for resin curing.

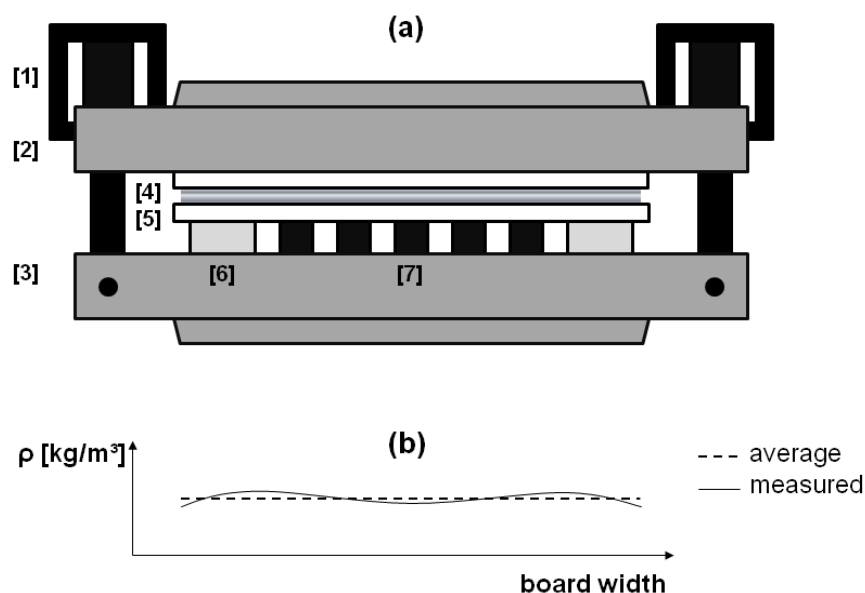


Fig. 1. a) Cross-section of the press frame of a continuous hot press with: [1] tie beam with main cylinder, [2] top press frame, [3] bottom press frame, [4] fiber mat, [5] press plate, [6] parallel support, [7] multi-pot system and b) its effect on average and measured density

In general, density variations across the width of the board are caused by different material distributions in the forming stage as well as material movement towards the edge zones during densification. Reduced density in the center of the board and higher density at the edge result from a different densification of the mat. According to Hse (1975), reduced density leads to reduced board strength. Considering the variation of board characteristics, it is evident why the average sample size for destructive tests must be relatively large (EN 326-2, 2000). The variation of board characteristics across the width of fiberboards has been analyzed by Hasener (2004) and Maschl (2009). Hasener (2004) found significant differences between the middle and the edge of boards by means of peeling tests and thickness swelling. However, internal bond strength (IB) and density were not significantly different at the testing positions across the width of boards. Additionally, a strong correlation between the density and the IB was found. Maschl (2009) analyzed 10 measurement points across the board width and detected no

significant differences for thickness swelling, whereas the IB, the modulus of rupture (MOR), and the modulus of elasticity (MOE) revealed significant differences between the metering points across the board width.

The mechanical properties (*e.g.* bending strength) of wood-based panels in the out-of-plane direction have been widely investigated using standard testing methods. Fracture tests for the analysis of wood-based panels in out-of-plane orientation have been performed by Ehart *et al.* (1996), Niemz and Diener (1999), Sinn *et al.* (2008), and Matsumoto and Nairn (2009).

As the quality control for the resin curing of wood-based panels must be performed in the core layer, the quality assurance tool has to ensure an in-plane measurement. Differences in the in-plane board direction (*i.e.* longitudinal and lateral to the feed direction) by means of fracture testing were analyzed by Matsumoto and Nairn (2009) and Rathke *et al.* (2012b). Matsumoto and Nairn (2009) did not find any differences in the in-plane orientation of MDF using extended compact tension specimens. When investigating oriented strand boards and particleboards that contain recycled wood chips, however, differences in the in-plane specimen orientation could be found by using the double cantilever I-beam (DCIB) approach (Rathke *et al.* 2012a). Nevertheless, no systematic trend was found as to whether longitudinal or lateral specimen orientation shows better performance, which makes measurements in both directions necessary.

For the analysis of wood-based panels, the elongated specimen geometry of the DCIB approach is well suited, as specimens are aligned either parallel or orthogonally to the production orientation. Moreover, fracture energy testing yields a higher number of parameters (*e.g.*, initial slope, fracture toughness, and specific fracture energy) than standard testing procedures. Therefore, this work investigates whether the DCIB approach can characterize mechanical differences across the board width more precisely than standard testing procedures.

MATERIALS AND METHODS

Specimen Preparation

In a central European HDF plant, a trial was performed to analyze interactions between raw material, resin, pressing temperature, various other process parameters, and the quality of HDF boards. HDF boards had a final thickness of 7.95 mm and were produced with a resin content of 15% (solid urea formaldehyde resin (UF) to oven dry fibers) and a paraffin content of 1.4 % (solid paraffin to oven dry fibers). In total, 23 boards were produced using individual process configurations. Samples were cut into specimen sets (*i.e.*, DCIB samples, IB samples, and bending strength/stiffness (BS) samples). Eight specimen sets, uniformly distributed over the board width, were cut from each board (Fig. 2). The measurements included both in-plane orientations of the wood based panels in production orientation (longitudinal) and across the production direction (lateral).

The specimens were stored in standard climate (*i.e.*, 20 °C and 65 % relative humidity (RH)) for two weeks, until equilibrium moisture content was achieved. Before further processing, the density of each specimen was determined by means of dimensional and gravimetric measurements (EN 323, 1993c). The calculation of the density ρ (in kg/m³) was performed according to Equation 1

$$\rho = \frac{m}{b_1 \cdot b_2 \cdot t} \cdot 10^6 \quad (1)$$

where m reflects the measured specimen weight (in gram), b_1 and b_2 describe length and width (in mm), respectively, while t stands for the specimen thickness (in mm).

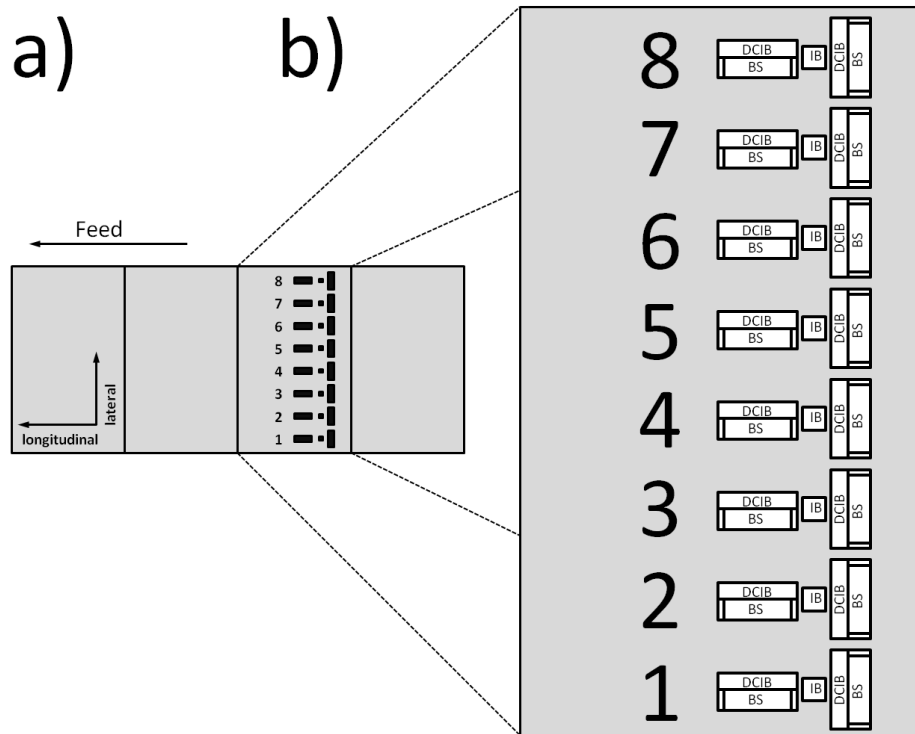


Fig. 2. Specimen selection: a) high density fiber boards were obtained from the industrial continuous production process and b) internal bond strength specimen (IB), double cantilever I-beam specimen (DCIB), and bending strength specimen (BS) were cut from industrially produced HDF boards in longitudinal and lateral orientation to the production process

IB analysis was carried out according to EN 319 (1993). Before testing, the IB specimens (50 mm × 50 mm) were bonded to aluminum loading blocks using a fast curing cyano-acrylate resin (Loctite 431, Henkel). The DCIB specimens had a length of 250 mm and a width of 24.5 mm (Fig. 3).

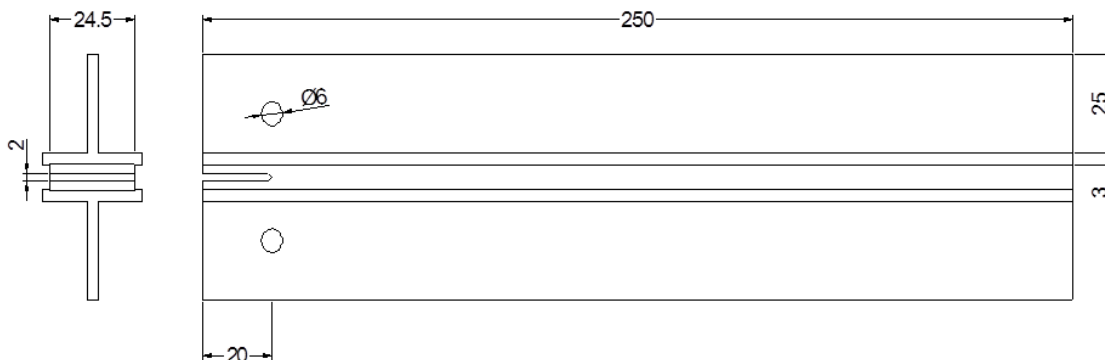


Fig. 3. Geometry of a double cantilever I beam (DCIB) specimen (all dimensions in mm)

An initial crack was sawn in the middle layer parallel to the panels' surfaces using a band saw (saw kerf-thickness 2 mm), to generate a notch with a depth of 19 mm in the core layer (Rathke *et al.* 2012a, b, c). Directly before testing, the notch was lengthened to a depth of 20 mm by means of a razor blade according to fracture tests performed by Stanzl-Tschegg *et al.* (1995) and Sinn *et al.* (2008). The specimens were glued to T-shaped braces made of steel using a fast curing cyano-acrylate adhesive (Loctite 431, Henkel).

The BS specimens were cut from HDF boards parallel to the DCIB specimens and had a dimension of 50 mm × 210 mm. After cutting, the specimens were tested without further treatment as described in EN 310 (1993b).

Internal Bond Strength Testing

The determination of IB according to EN 319 (1993) was performed on a Zwick/Roell Z020 universal testing machine, equipped with a 2.5 kN load cell. The specimens were tested with a crosshead speed of 0.5 mm/min. Failure occurred within 60 ± 30 s after applying a pre-force of 20 N. The IB (in MPa) was calculated according to Equation 2 by dividing the maximum load F_{max} by the base area ($a \cdot b$) of the specimen.

$$IB = \frac{F_{max}}{a \cdot b} \quad (2)$$

Fracture Energy Testing

The fracture tests were performed on a Zwick/Roell Z100 universal testing machine equipped with a 2.5 kN load cell. Fracture energy testing requires a tensile load perpendicular to the area in the middle layer of boards, which leads to fracture in mode I. The specimens were clamped into fasteners with pins and a load was applied at the notched end of the specimen (Fig. 3), leading to stresses within the specimen. The ground of the initial notch was half the distance of the connecting line between the upper and the lower pin boreholes to permit the application of direct force. A crosshead speed of 1 mm/min was chosen. After reaching a force drop of 50 % of the maximum load, the crosshead speed was continually increased up to 10 mm/min. Similar to IB testing, the maximum load was reached within 60 ± 30 s (CEN 1993b). The test was stopped after a maximum displacement of 50 mm or a remaining force of 5 N. These settings guaranteed testing periods of 3 min at the most.

The fracture energy was calculated by integrating the area below the load-displacement curve (Fig. 4).

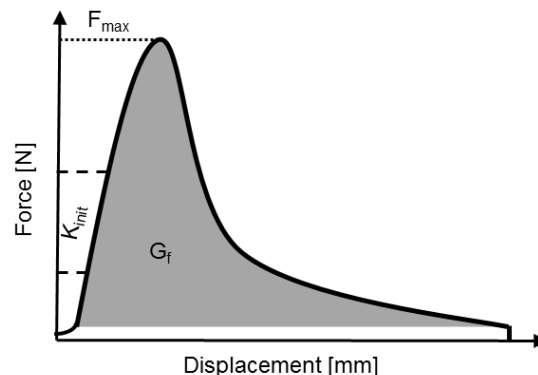


Fig. 4. Load-displacement curve of Double Cantilever I-Beam testing

The results reflect the fracture work that is necessary to split specimens into two parts. According to Hu and Wittmann (1992), the specific fracture energy G_f (in J/m²) is the applied energy in a stable or quasi-stable fracture of a notched specimen, averaged over the fractured area. Accordingly, the specific fracture energy (in J/m²) can be calculated by relating the fracture work to the fracture area (Equation 3),

$$G_f = \frac{1}{(L-a)B} \int_0^{z_{max}} F dz \quad (3)$$

where F is the applied force, z is the displacement at the loading point, a indicates the initial crack length, and L and B are the total length and the width of the specimen, respectively.

Tabulated formulas for the stress intensity factors are based on the assumptions of an isotropic material and simple geometry. In order to determine the critical stress intensity factor K_{IC} (in MPa m^{1/2}) in mode I, material tests were performed and the data were used for a finite-element-method (FEM) simulation with the software ABAQUS®. The problem was reduced to a two-dimensional, plain strain model. The J-Integral stress intensity factor algorithm from ABAQUS® was used to derive Equation 3 from simulations with an adjustable isotropic modulus of elasticity of the board. A precise description of the FEM – simulation is given in Rathke *et al.* (2012a, d). The relative error between FEM-simulation and Equation 4 is less than 0.5 % for $3.165 < \frac{k_{init}}{b} < 1100$,

$$K_{IC} = F_{max} [(6.568E - 05) + (2.082E - 7) \cdot \frac{k_{init}}{b} + (-1.498E - 10) \cdot (\frac{k_{init}}{b})^2 + (5.253E - 14) \cdot (\frac{k_{init}}{b})^3] \quad (4)$$

where F_{max} reflects the maximum applied load, k_{init} is the initial slope, and b is the specimen width.

Bending Stiffness and Strength

Flatwise three-point bending tests were performed, corresponding to EN 310. Samples with dimensions of 210 mm × 50 mm × 7.95 mm ($l \times b \times t$) were tested using a Zwick/Roell Z100 universal testing machine with a crosshead speed of 7.5 mm/min. The specimen thickness resulted in a free span length l_1 of 210 mm. To exclude the layering effects of the face and bottom layers, every second specimen was tested upside down. Specimen failure occurred within 60 ± 30 s after an applied pre-force of 10 N. The calculation of the modulus of elasticity (MOE in MPa) is given in Equation 5 (EN 310),

$$MOE = \frac{l_1^3 (F_2 - F_1)}{4 b t^3 (a_2 - a_1)} \quad (5)$$

where $F_2 - F_1$ describes the force increase in the linear elastic part of the force-deflection graph. F_1 is the force at 10% of the maximum load, while F_2 denotes 40% thereof. The variables a_1 and a_2 are the corresponding deflections to F_1 and F_2 . The bending strength (modulus of rupture) MOR (in MPa) was calculated as described in Equation 6,

$$MOR = \frac{3 F_{max} l_1}{2 b t^2} \quad (6)$$

where F_{max} stands for the maximum load. The variables l_1 , b , and t stand for the same numbers as described in the calculation of the MOE in Equation 5.

RESULTS AND DISCUSSION

The results of the density determination and the IB testing are presented in Fig. 5. Figure 6 shows the results of mechanical testing at eight positions across the width of the board, both longitudinally and laterally to the production direction. For statistical analysis, a one-way analysis of variance (ANOVA, $p < 0.05$) was performed, followed by a subsequent multiple t-test with Bonferroni procedure, using SPSS®.

Density and Internal Bond Strength

A comparison of the density at metering points across the width of the board, using IB specimens, yielded significant differences ($p = 0.001$) between metering points 1 and 7. In general, the pattern of density across the width of boards is assumed to be symmetric, with two peaks at the edge zones. However, the values in Fig. 5 show only one peak at metering point 7, while the metering points 1 and 2 at the opposite edge had the lowest density of all metering points. Nevertheless, this could be explained by a systematic asymmetric distribution of fibers at the forming stage, when the mat is formed. The density of all specimens varied with a coefficient of variation (CV) of 0.02 on average.

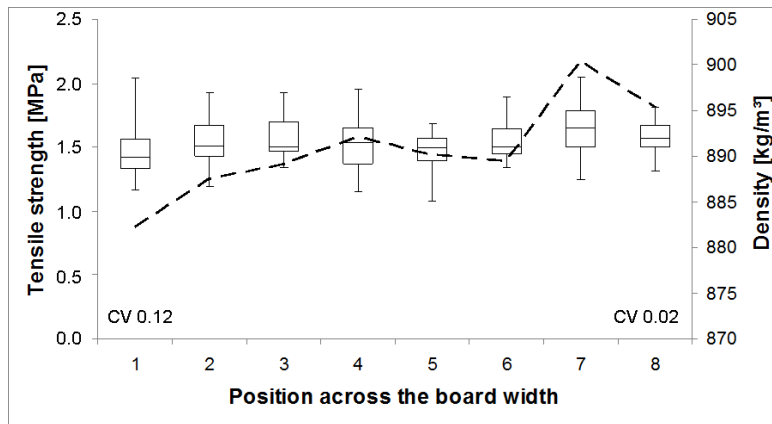


Fig. 5. Results of internal bond strength measurements (box-plots) and density analysis (dashed line) with mirrored density profile line due to mechanical defect in the fiber distribution unit of the HDF plant (red dashed line) and CV values

The internal bond strength tests revealed significant differences in the metering pairs 1 and 7 ($p = 0.001$) and 5 and 7 ($p = 0.02$). The mean CV of all IB specimens was 0.12, which is within a normal range. The high IB values for metering point 7 and the low IB values for metering point 5 are characteristic of a board cross-section, in contrast to the low IB values for metering point 1. A probable explanation for the low IB values for the metering points 1 and 2 is the lower density at these points, as the coefficient of correlation (R) between density and IB was 0.55. These findings are contrary to those of Hasener (2004), who did not detect any significant differences in density and IB in relation to their position across a board. In contrast, Maschl (2009) found significant differences between the IB values at the edge zone and at the center of the board.

Mechanical Testing Results from Specimen with Elongated Geometry

The specific fracture energy (G_f) determined by the DCIB testing procedure did not yield significant differences in the lateral orientation of specimens due to the homogenizing effect of the elongated shape of specimens. In contrast, significant differences were found in the longitudinal orientation, *i.e.*, with specimens aligned in the production direction. The central metering point 4 was significantly different from the edge zone metering points 7 and 8. In contrast, the metering points 1 and 2, from the opposite edge zone, did not yield significant differences when compared to the central metering points.

By analyzing the values of the stress intensity factor (K_{IC}), significant differences were found between the metering points 5 and 8 for the longitudinally orientated specimens (Fig. 6). Laterally orientated, the metering points 4 and 5 were significantly different from the metering point 7 in the edge zone (Fig. 6).

In lateral orientation, the MOE showed no significant differences between metering points. In contrast, the longitudinal orientation showed significant differences between the metering points 3 and 4 and the edge zone at point 8. While IB, G_f , and K_{IC} appeared to have lower values in the center of the board than at the edges, the MOE showed the opposite behavior (Fig. 6). MOR did not reveal significant differences between the metering points across the board in both longitudinal and lateral specimen orientations. However, bending properties (MOE, MOR) qualitatively showed a trend towards higher testing results in the center of the board. The higher values were probably due to stronger and stiffer board faces in middle positions.

The CV was calculated over the entire width of the board, including all specimens. This was performed with both longitudinal and lateral specimen orientation. The usage of the CV enables a comparison of all testing systems. MOE, MOR, and density had the lowest CV values. The CV of the IB ($CV = 0.12$) and the CV of the K_{IC} ($CV_{long} = 0.13$; $CV_{lat} = 0.12$) were within the same range, which indicates that both had a similar accuracy of reproducibility. The G_f in lateral orientation showed the highest variation from the mean with a CV of 0.26. This high CV was attributed to the scattering of data within the groups of every single metering point. One possible explanation is the higher variation of density across the width of the board compared to the variation of density in longitudinal direction due to physical processes at the hot pressing process. A second explanation could be the size and orientation of DCIB specimens, which result in higher scattering of data for laterally oriented specimens than for specimens that were longitudinally oriented. Nevertheless, DCIB testing showed significant differences between the edge and center parts of the board.

Pearson's coefficient of correlation between the density and the mechanical properties of specimens with elongated geometry were significant in longitudinal and lateral specimen orientations. The correlation between density and G_f in lateral direction was $r^2 = 0.13$, and between density and MOE in lateral direction $r^2 = 0.17$. These low values can be explained by the density variations in the core layer, especially in lateral orientation. Results with better correlations were found between density and lateral measured values for K_{IC} ($r^2 = 0.3$) and MOR ($r^2 = 0.31$).

The correlation between density and G_f in longitudinal direction was $r^2 = 0.25$. The correlation between density and mechanical testing in longitudinal specimen orientation for K_{IC} was $r^2 = 0.31$, for MOE $r^2 = 0.35$, and for MOR $r^2 = 0.3$. Consequently, a better correlation between mechanical parameters and density was gained from longitudinally oriented specimens. The higher CV values of mechanical properties in longitu-

dinal specimen orientation (with the exception of G_f) indicate a higher explanatory power in this orientation and should therefore be preferred.

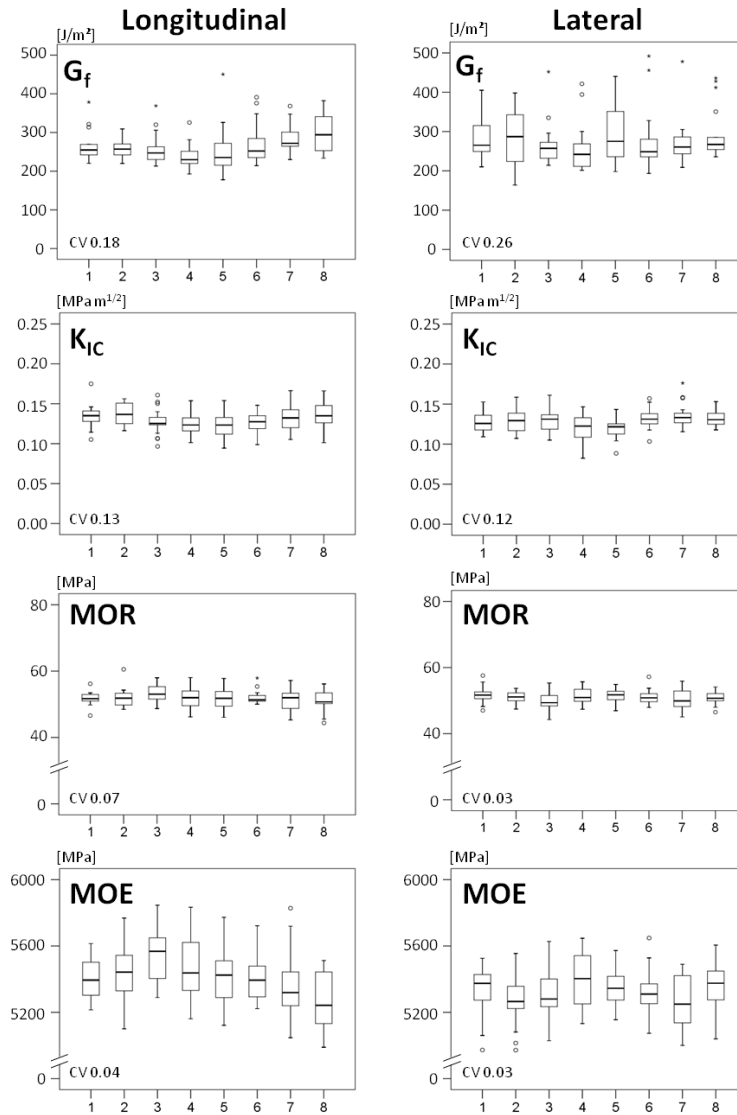


Fig. 6. Results of specific fracture energy (G_f), stress intensity factor (K_{IC}), modulus of rupture (MOR), and modulus of elasticity (MOE) for high density fiberboards across the width of the board with specimen orientation in production direction (longitudinal) on the left side and orthogonal to the production direction (lateral) on the right side

CONCLUSIONS

1. The in-plane layering effects (*i.e.* longitudinal and lateral) on the mechanical properties across the width of HDF had no effect on the modulus of rupture, which was uniform across the width of the board.
2. The internal bond strength and the modulus of elasticity, as well as the G_f and K_{IC} obtained from the newly developed double cantilever I-beam approach, revealed

significant differences between one of the edges and center parts of boards (asymmetric behavior). Thus, the DCIB approach is appropriate for detecting differences across the width of HDF.

3. A comparison of the data in longitudinal and lateral orientation showed that a higher explanatory power was achieved in production direction than orthogonal to it, especially with the elongated DCIB specimen geometry.
4. With regard to quality assurance, it is assumed that if the variations across the width of the board were taken into account, the number of samples needed per process control step could be reduced.

REFERENCES CITED

- Bouajila, J., Limare, A., Joly, C., and Dole, P. (2005). "Lignin plastification to improve binderless fiberboard mechanical properties," *Polymer Engineering and Science* 45(6), 809-816.
- Cao, J., Zhang, X., and Liu, Y. (2007). "Fuzzy control of medium density fiberboard hot-pressing," *Proceedings of the 2nd IEEE Conference on Industrial Electronics and Applications, ICIEA, Harbin, China, 2045-2048*.
- Carvalho, L. M. H., Costa, M. R. N., and Costa, C. A. V. (2001). "Modeling rheology in the hot-pressing of MDF: Comparison of mechanical models," *Wood and Fiber Science* 33(3), 395-411.
- CEN (1993a). "EN 310: Wood-based-panels – Determination of modulus of elasticity in bending and of bending strength," Österreichisches Normungsinstitut, Vienna, Austria.
- CEN (1993b). "EN 319: Particleboards and fiberboards – Determination of tensile strength perpendicular to the plane of the board," Österreichisches Normungsinstitut, Vienna, Austria.
- CEN (1993c). "EN 323: Wood-based-panels – Determination of density," Österreichisches Normungsinstitut, Vienna, Austria.
- CEN (2000). "EN 326-2: Wood-based-panels – Sampling, cutting and inspection," Österreichisches Normungsinstitut, Vienna, Austria.
- Dunky, M., and Niemz, P. (2002). *Holzwerkstoffe und Leime*, Springer, Berlin, Heidelberg, New York, 856.
- Ehart, R. J. A., Stanzl-Tschegg, S. E., and Tschegg, E. K. (1996). "Characterization of crack propagation in particleboard," *Wood Science and Technology* 30(5), 307-321.
- Hasener, J. (2004). "Statistische Methoden der industriellen Prozessmodellierung zur Echtzeitqualitätskontrolle am Beispiel einer kontinuierlichen Produktion von Faserplatten," PhD Thesis, University Hamburg, Hamburg, Germany.
- Heinemann, C. (2004). "Charakterisierung der Aushärtung von Aminoharzen in einer Holzpartikelmatrix durch Evaluierung von Festigkeiten und Reaktionskinetik," PhD Thesis, University Hamburg, Department of Biology, Hamburg, Germany.
- Hse, C.-Y. (1975). "Properties of flakeboards from hardwoods growing on southern pine sites," *Forest Products Journal* 25(3), 48-53.
- Hu, X.-Z., and Wittmann, F. H. (1992). "Fracture energy and fracture process zone," *Materials and Structures* 25(6), 319-326.

- Maschl, G. (2009). "Improvement of fiberboard manufacture through statistical process analytics," Master's Thesis, University of Natural Resources and Life Sciences Vienna, Department of Material Sciences and Process Engineering, Vienna, Austria.
- Matsumoto, N., and Nairn, J. (2009). "The fracture toughness of medium density fiberboard (MDF) including the effects of fiber bridging and crack-plane interference," *Engineering Fracture Mechanics* 76(18), 2748-2757.
- Maxwell, J. W., Gran, G., and Waters, G. D. (1984). "Experiments with blowline blending for MDF," *Proceedings of the Eighteenth Washington State University International Particleboard/Composite Materials Series Symposium*, Washington State Univ., Pullman, Washington, USA, 117-143.
- Niemz, P., and Diener, M. (1999). "Vergleichende Untersuchung zur Ermittlung der Bruchzähigkeit an Holzwerkstoffen," *Holz als Roh- und Werkstoff* 57(3), 222-224.
- Park, B.-D., Riedl, B., Hsu, E. W., and Shields, J. (1999). "Hot-pressing process optimization by response surface methodology," *Forest Products Journal* 49(5), 62-68.
- Pereira, C., Carvalho, L. M. H., and Costa, C. A. V. (2006). "Modeling the continuous hot-pressing MDF," *Wood Science and Technology* 40(4), 308-326.
- Rathke, J., Sinn, G., Weigl, M., and Müller, U. (2012a). "Analysing in-plane orthotropy of wood based panels by means of fracture mechanics," *European Journal of Wood and Wood Products* 70(6), 851-856.
- Rathke, J., Sinn, G., Harm, M., Teischinger, A., Weigl, M., Müller, U. (2012b). "Fracture energy vs. internal bond strength—Mechanical characterization of wood-based panels," *Wood Material Science and Engineering* 7, 1-10.
- Rathke, J., Sinn, G., Harm, M., Teischinger, A., Weigl, M., Müller, U. (2012c). "Effects of raw material, particle geometry and resin content on mechanical properties of particle board," *BioResources* 7, 2970-2985.
- Rathke, J., Sinn, G., Konnerth, J., Müller, U. (2012d). "Strain measurements within fibre boards. Part III: Analysing the process zone at the crack tip of MDF Double Cantilever I-Beam specimens," *Materials* 5, 2190-2204
- Roffael, E., Dix, B., Schneider, T., and Kraft, R. (2003). "Extractable urea in MDF prepared using the blowline- and blender-technique," *Holz als Roh- und Werkstoff* 61(1), 73-74.
- Roffael, E., Schneider, T., and Dix, B. (2005). "On paraffin sizing of medium density fiberboards (MDF) Part 2: Influence of resination process (blender and blowline technique) and method of adding paraffin dispersion within the blender- and blowline-process on paraffin sizing of medium density fibreboards (MDF)," *Holz als Roh- und Werkstoff* 63(4), 272-277.
- Sinn, G., Beer, P., Gindl, M., and Stanzl-Tschegg, S. (2008). "Wedge splitting experiments on three-layered particleboard and consequences for cutting," *Holz als Roh- und Werkstoff* 66, 135-141.
- Stanzl-Tschegg, S. E., Tan, D. M., and Tschegg, E. K. (1995). "New splitting method for wood fracture characterization," *Wood Science and Technology* 29, 31-50.
- Walther, T. (2006). "Methoden zur qualitativen und quantitativen Analyse der Mikrostruktur von Naturfaserwerkstoffen," PhD Thesis, University Hamburg, Department of Biology, Hamburg, Germany.
- Wang, S., Winistorfer, P. M., Young, T. M., and Helton, C. (2001). "Step-closing pressing of medium density fiberboard: Part 2. Influences on panel performance and layer characteristics," *Holz als Roh- und Werkstoff* 59(5), 311-318.

Waters, G. D. (1990). "Medium density fibreboard blowline blending theories in and around the Black Box," *Proceedings of the NPA Resin and Blending Seminar*, Irving Texas, USA.

Article submitted: January 20, 2013; Peer review completed: April 25, 2013; Revised version accepted: June 3, 2013; Published: June 5, 2013.